Electron-phonon coupling in the undoped cuprate YBa_{2}Cu_{3}O_{6} estimated from Raman and optical conductivity spectra

D. Farina, G. De Filippis, A. S. Mishchenko, N. Nagaosa, Jhih-An Yang, D. Reznik, Th. Wolf, and V. Cataudella

Phys. Rev. B **98**, 121104 — Published 11 September 2018

DOI: 10.1103/PhysRevB.98.121104

Electron-phonon coupling in undoped cuprate $YBa_2Cu_3O_6$ estimated from Raman and optical conductivity spectra

D. Farina,[1,2] G. De Filippis,[3] A. S. Mishchenko,[4,5] N. Nagaosa,[4,6]
Jhih-An Yang,[7] D. Reznik,[7,8] Th. Wolf,[9] and V. Cataudella[3]

[1]*Scuola Normale Superiore, Piazza dei Cavalieri 7, I-56126, Pisa, Italy*
[2]*Istituto Italiano di Tecnologia Center for Nanotechnology Innovation @NEST Piazza San Silvestro 12, 56127 Pisa , Italy*
[3]*SPIN-CNR and Dip. di Scienze Fisiche - Università di Napoli Federico II - I-80126 Napoli, Italy*
[4]*RIKEN Center for Emergent Matter Science (CEMS), 2-1 Hirosawa, Wako, Saitama, 351-0198, Japan*
[5]*NRC "Kurchatov Institute", 123182, Moscow, Russia*
[6]*Department of Applied Physics, The University of Tokyo, 7-3-1 Hongo, Bunkyo-ku, Tokyo 113, Japan*
[7]*Department of Physics, University of Colorado-Boulder Boulder, CO 80309, USA*
[8]*Center for Experiments on Quantum Materials, University of Colorado-Boulder, Boulder, Colorado, 80309, USA*
[9]*Institute for Solid State Physics, Karlsruhe Institute of Technology, D-76021 Karlsruhe, Germany*

We study experimentally the Raman response of the undoped high-T_c parent compound $YBa_2Cu_3O_6$, and give a unified theory of the two-magnon Raman peak and optical conductivity based on the Hubbard-Holstein model with electron-phonon coupling (EPC). The Hubbard model without EPC can qualitatively account for the experimentally observed resonance of the Raman response, but only the Hubbard-Holstein model (i) reproduces asymmetry of the Raman spectrum, (ii) validates experimental visibility of the two-magnon peak, and (iii) predicts the correct shape and energy of the lower edge of the charge transfer gap in optical conductivity. Comparison of experiments with the theory gives the EPC strength $\lambda = 0.6$. This result convincingly indicates the vital role of EPC in high-Tc cuprates providing a clue to the mechanism of high-T_c.

PACS numbers: 71.38.-k, 72.20.Fr, 02.70.Ss

High critical temperature (high-T_c) superconductivity is the phenomenon whose understanding is not only a challenge for descriptive power of the modern theoretical concepts but also bears immense importance for potential numerous applications in many fields of innovative technology. In spite of enormous efforts to understand the physics of high-T_c there is no adopted opinion on the driving forces leading to the superconducting transition yet[1]. Moreover, there is even no consensus on which types of interactions are crucial for the description of the normal state of high-T_c compounds. It has been adopted by most that the unusual superconductivity of high-T_c compounds cannot be described by conventional Bardeen-Cooper-Schrieffer (BCS) mechanism based on the electron-phonon coupling (EPC) and, hence, one has to assume an important role of the electron-electron interaction (EEI). The emphasis on the EEI in a majority of considered theoretical concepts puts the EPC out of the picture leaving an impression that the EPC does not play any role in the physics of high-T_c materials.

However, it has been shown by recent studies that the EPC manifests itself in many phenomena[2–11] and it was concluded that one needs both EEI and EPC to describe high-T_c materials[12,13]. The main class of unconventional superconductors are cuprates whose parent undoped compounds are in the Mott insulating antiferromagnetic (AF) state. Doping of these compounds by holes destroys AF state and induces superconductivity. Recent theoretical studies based on nonperturbative approaches established that the EPC is strongly reflected in spectroscopy of undoped and weakly doped compounds though its manifestations weaken with hole doping[10,14].

Hence, to address the role of EPC, we focus on undoped compounds where EPC is manifested most clearly, as the basis to construct the theoretical model describing cuprates. This enables the quantitative estimate of the strength of EPC.

To verify the importance of EPC, we calculated the polarization-resolved two-magnon Raman spectrum (RS) and optical conductivity (OC) of the undoped ($\delta = 0$) $YBa_2Cu_3O_{6+\delta}$ (YBCO) which is one of the reference high-T_c materials. Our calculations show that solely EEI-based description, using model parameters required to describe angle resolved photoemisson spectra of high-T_c compounds, is not successful whereas inclusion of rather substantial EPC not only improves description of both RS and OC but provides a unique possibility to describe both experimental responses within the same unified model.

Model. EEI is introduced in the framework of the extended two-dimensional effective one-band Hubbard model which has been derived elsewhere[15,16] from the more general three band description. In addition, we will take into account the coupling between the charge carriers and the vibrational modes of the lattice. The Hamiltonian is:

$$H = H_{\rm H} + H_{\rm PH} + H_{\rm EPC} \, . \qquad (1)$$

The first term describes pure electronic system with the strong on site Hubbard Coulomb repulsion U, nearest neighbor coupling constant V, and next nearest neighbor constant V'

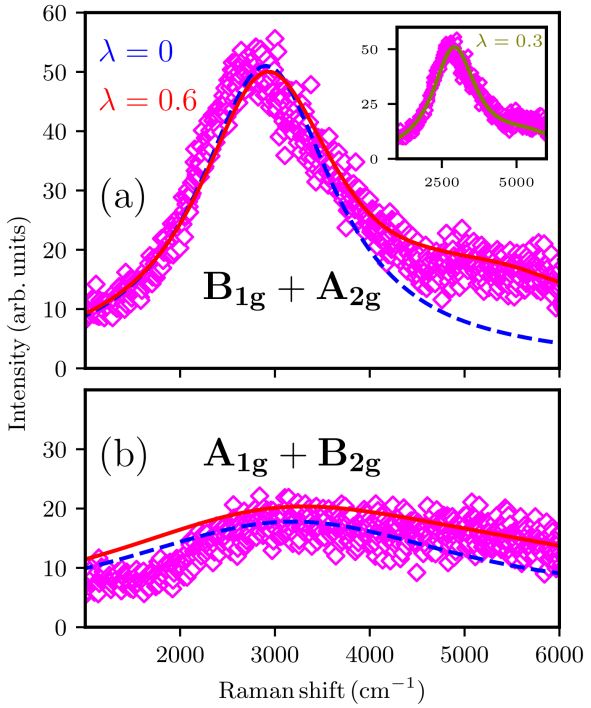

FIG. 1. (color online) Calculated Raman signal in (a) B_{1g}+A_{2g} and (b) A_{1g}+B_{2g} symmetries without (dash blue line) and with (solid red line) EPC ($\lambda = 0.6$). In the inset calculated Raman signal in B_{1g}+A_{2g} symmetry at $\lambda = 0.3$. Experimental data shown by diamonds were obtained on a single crystal sample of insulating $YBa_2Cu_3O_{6+x}$ using 3.05eV incident laser energy on the McPherson triple Raman spectrometer at 300K.

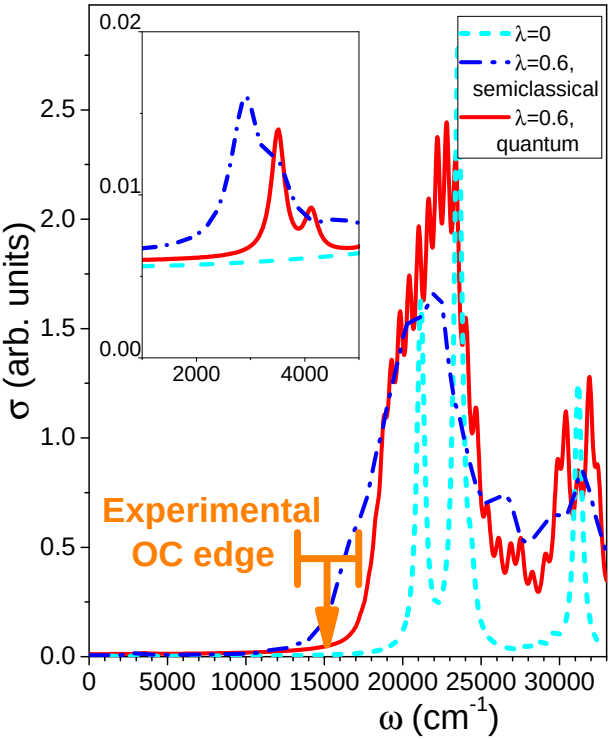

FIG. 2. (color online) Theoretical optical conductivity at $\lambda = 0$ (cyan dashed line) and at $\lambda = 0.6$ within the semiclassical (blue dash-dotted line) and quantum (red solid line) approaches for phonons. The range of OC edge observed in experiments (12100cm^{-1}-16100cm^{-1}) is given by orange error-bar with orange arrow. Inset shows comparison of OCs in the low-energy window.

$$H_{\rm H} = -t\sum_{i,\delta,\sigma} c^\dagger_{i+\delta,\sigma}c_{i,\sigma} + U\sum_i n_{i,\uparrow}n_{i,\downarrow} + V\sum_{i\delta\sigma\sigma'} n_{i+\delta\sigma}n_{i\sigma'} + V'\sum_{i\delta'\sigma\sigma'} n_{i+\delta'\sigma}n_{i\sigma'}. \quad (2)$$

The vibrational subsystem is described by the out-of-plane dispersionless phonon of apical oxygen ions in YBCO:

$$H_{\rm PH} = \omega_0\sum_i a^\dagger_i a_i\ . \quad (3)$$

These couple to charge fluctuations

$$H_{\rm EPC} = g\omega_0\sum_i (n_i - 1)\,(a^\dagger_i + a_i) \quad (4)$$

by on-site Holstein type EPC whose strength is characterized by dimensionless 2D coupling constant $\lambda = g^2\omega_0/(4t)$. The values of the parameters entering Eq.(1) have been chosen in agreement with the literature[17–19]. In the present paper we adopt $t = 0.36eV$, $U = 10t$, $\omega_0 = 0.2t$, $V = 0.2U$, $V' = 0.1U$ (V and V' have been chosen by assuming a Youkawa-like electron-electron potential)[20]. The antiferromagnetism is controlled by the Heisenberg exchange energy, $J = 4t^2/U$, that turns out to be $J = 0.4t$. To calculate the optical response we used exact diagonalization of small systems with semiclassical phonon in adiabatic approximation (Raman and OC) and with quantum phonons (OC) (see the Supplemental Material[20]). To learn about the importance of EPC we compared theoretical description with ($\lambda = 0.6$) and without ($\lambda = 0$) EPC. We emphasize that the value $\lambda = 0.6$ restores the correct behavior of OC at very low dopings[30].

Properties where EPC is crucial for describing experiments. In polarization-resolved Raman response we focused on the bimagnon peak (2M-peak) which is located at Raman shift $\omega = \omega_L - \omega_S$ around $3000cm^{-1}$[21–23]. This shift is the energy loss between incoming laser light with frequency ω_L and outgoing light frequency ω_S. The adopted explanation of the nature of 2M-peak is given by Chubukov-Frenkel theory[24]. According to this theory the incident light ω_L creates electron-hole pair through the electronic gap which is followed by emission of two bound magnons with the opposite momenta decreasing electron-hole pair energy by ω. Consequent recombination leads to emission of light with smaller frequency ω_S

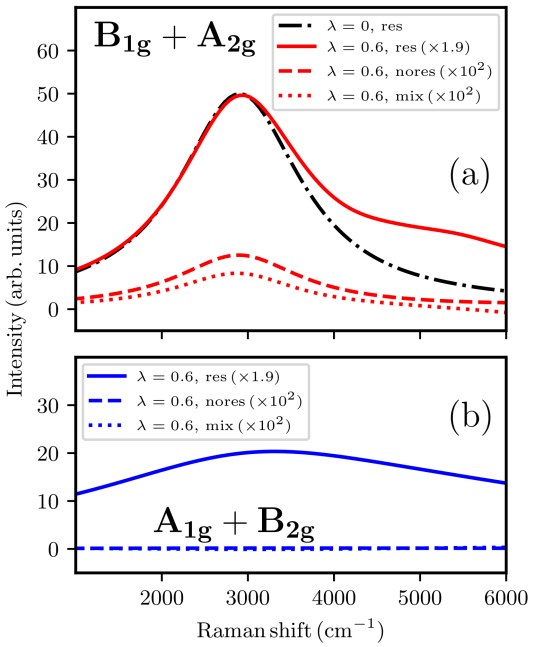

FIG. 3. (color online) Resonant (solid line), mixed (dotted line), and non-resonant (dash line) contributions to the Raman response in (a) $B_{1g} + A_{2g}$ and (b) $A_{1g} + B_{2g}$ symmetries with electron-phonon interaction ($\lambda = 0.6$) for incoming laser frequency $\omega_L = 25250\text{cm}^{-1}$. Resonant contribution at $\lambda = 0$ is given in panel (a) by black dotted line.

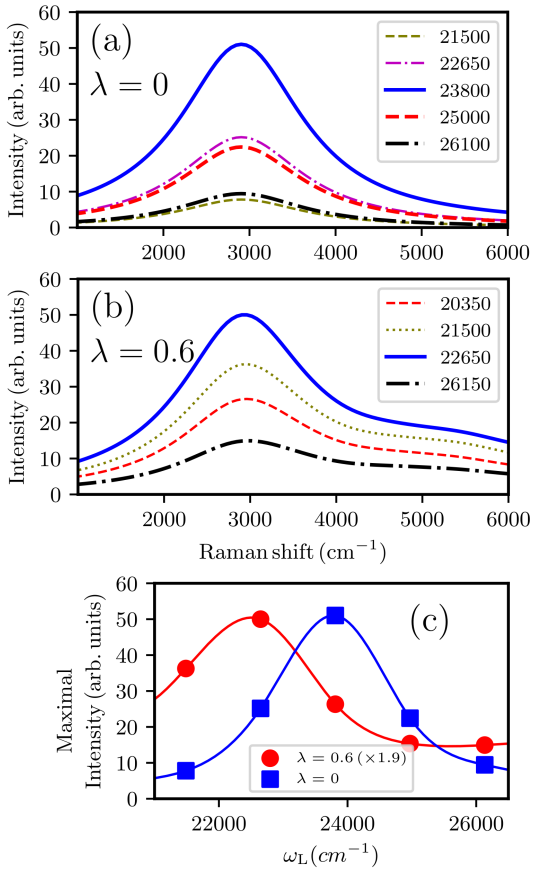

FIG. 4. (color online) Resonant behavior of Raman response in $B_{1g} + A_{2g}$ symmetry (a) without and (b) with electron-phonon coupling ($\lambda = 0.6$). The incoming laser frequencies ω_L in cm^{-1} are given in figure legends. Panel (c) shows dependence of the maximal Raman signal intensity on the incoming laser frequency ω_L.

than incoming light by Raman shift ω. This process is resonant and the intensity of 2M-peak increases when either ω_L matches the upper edge or when ω_S matches the lower edge of the electronic gap[25,26].

The energy of 2M-peak is mainly determined by EEI whereas, as shown in Fig. 1, introduction of EPC significantly improves similarity of the theoretical description of the Raman response to that measured in experiment[27]. The bimagnon excitation is most pronounced in the Raman response in the $B_{1g} + A_{2g}$ channel where B_{ng} and A_{ng} are irreducible representations of the YBCO crystal point group D_{4h}. This is experimentally detectable by Raman spectroscopy in the $x'y'$ polarization configuration when the incoming $\mathbf{e}_L$ and outgoing $\mathbf{e}_S$ photon polarizations are perpendicular to each other and oriented at 45° with respect to the 2D lattice bonds. The complementary symmetry $A_{1g} + B_{2g}$ or $x'x'$ is experimentally obtained by rotating $\mathbf{e}_S$ to make it parallel to $\mathbf{e}_L$ along the x' direction.

Without the EPC, in severe contrast with experimental data[23,28], the theoretical 2M-peak in the $B_{1g} + A_{2g}$ channel is perfectly symmetric with respect to the bimagnon energy $\omega_{2M} \sim 2.5J \approx 3000\text{cm}^{-1}$. Inclusion of the EPC cures this discrepancy between the theory and experiment and quantitatively reproduces the asymmetry, see Fig. 1a (inset in Fig. 1a points out that the best agreement with experimental observations is obtained at $\lambda = 0.6$). On the other hand EPC plays a minor role in the $A_{1g} + B_{2g}$ symmetry (see Fig. 1b). However, also in this case, the agreement with experimental observations is improved by the inclusion of charge lattice coupling.

As for the OC, the very visibility of the 2M-peak in the theoretical description is the consequence of EPC, see inset in Fig. 2. Intensity of 2M-peak in rigid YBCO is suppressed by the point inversion symmetry of the unit cell and only EPC makes the 2M-peak visible in principle because phonons break this high symmetry. We note that although the intensity of the bimagnon peak in OC is orders of magnitude weaker than the spectral weight above the gap[29,30], the very presence of this signal, observed in experiment[31], is an unambiguous proof of the importance of EPC.

Inclusion of EPC provides other important improvements concerning the shape and the value of the gap in the OC, see Fig. 2. Indeed, in the ground state at half-filling, Coulomb repulsion forces the electrons to localize, freezing charge fluctuations. In such a state, the

coupling between localized fermions and bosonic excitations, which is mediated by charge dynamics, is strongly suppressed. On the other hand, at the edge of OC, where holons and doublons are formed, charge lattice coupling becomes relevant. EPC moves the edge of the OC to lower energies building up a characteristic tail just as reproduced by experiments[32–34]. Here the main role is played by excitons strongly dressed by phonons. On the other hand, the effect of phonons is less important well inside the absorption band where no polaron can be formed. Nevertheless a simple broadening of the peaks is observed above the charge transfer gap too.

Properties where EPC is not crucial but plays a big role. Here we discuss the properties, which are not substantially modified by the inclusion of EPC. To this aim one has to consider the structure of Raman response and OC. The exact eigenstates representation for the polarization-resolved electronic Raman spectrum at zero temperature as a function of the Raman shift $\omega \equiv \omega_L - \omega_S > 0$, is given by[35,36]

$$I_{Raman}(\omega; \mathbf{e}_L, \mathbf{e}_S) \propto \frac{\omega_S}{\omega_L} \sum_f |\langle \Psi_f | \mathbf{e}_S^\dagger M \mathbf{e}_L | \Psi_0 \rangle|^2 \times \Im \frac{1}{\omega - E_f + E_0 - i\epsilon} \quad (5)$$

where $\mathbf{e}_L$ and $\mathbf{e}_S$ are polarizations of the incoming and outgoing light, E_0 and $|\Psi_0\rangle$ are energy and wave function of the ground state, and E_f and $|\Psi_f\rangle$ are energies and wave functions of the final states. The matrix elements of the Raman scattering tensor operator

$$\langle \Psi_f | M_{lm} | \Psi_0 \rangle = \langle \Psi_f | \tau_{lm} | \Psi_0 \rangle + \sum_r \left\{ \frac{\langle \Psi_f | j_l | \Psi_r \rangle \langle \Psi_r | j_m | \Psi_0 \rangle}{\omega_L + E_0 - E_r - i\eta} - \frac{\langle \Psi_f | j_m | \Psi_r \rangle \langle \Psi_r | j_l | \Psi_0 \rangle}{\omega_L + E_r - E_f - i\eta} \right\} \quad (6)$$

contain two contributions. The first term is non-resonant, is determined by the Raman stress tensor operator τ_{lm} (see the Supplemental Material[20]), and is insensitive to the incoming photon frequency ω_L. The second one strongly depends on the frequency ω_L, which can resonate only with the difference of the energies of the intermediate $|\Psi_r\rangle$ and ground states, $E_r - E_0$, because of total energy conservation. The resonant term contains the components of the current operator j_l (see the Supplemental Material[20]), and the intermediate states $|\Psi_r\rangle$. The particular structure of the Raman response makes it much more sensitive to symmetry breaking than OC[37,38], namely to degenerate eigenvalues of the system Hamiltonian. The expression for OC reads as follows

$$\Re \sigma_{xx}^{reg}(\omega) = \sum_{n \neq 0} \frac{|\langle \Psi_n | j_x | \Psi_0 \rangle|^2}{E_n - E_0} \times \Re \left[i \left(\frac{1}{\omega + i\delta - E_n + E_0} - \frac{1}{\omega + i\delta + E_n - E_0} \right) \right]. \quad (7)$$

The dominant contribution to the Raman scattering, both with and without EPC, comes from the resonant contribution, see Fig. 3 where different terms of the Raman response are compared for $\lambda = 0.6$. Fig. 3a compares resonant contributions at $\lambda = 0.6$ and $\lambda = 0$. One can conclude that the EPC is responsible for the experimentally observed asymmetry of the 2M-peak in $B_{1g} + A_{2g}$ symmetry and that EPC mostly affects the resonant contribution. This stems from the observation that the resonant contribution involve states at the edge of OC, where holons and doublons are formed and EPC plays a significant role.

The resonant behavior is observed both with and without EPC (Fig. 4). In both cases, comparing Fig. 4c and Fig. 2, one concludes that the resonant contribution is maximal when the incident frequency ω_L matches the maximum of the OC above the charge transfer gap. However, the resonance is much broader when EPC is included, which is closer to the experiment[39].

We emphasize that RS are often discussed in literature within the framework of the Fleury-London theory based on the coupling between the light and the spin system in the Heisenberg model[40]. However these approaches do not reproduce resonant scattering occurring when the frequency of the incoming light is comparable to the charge transfer gap. In order to recover the experimental resonance one has to take into account the full Hubbard model[17].

Conclusion. We compared the capabilities of the extended Hubbard and extended Hubbard-Holstein models to give a unified description of the Raman response and optical conductivity of high-T_c superconductors on the example of the prototypical undoped compound ($\delta = 0$) $YBa_2Cu_3O_{6+\delta}$. We showed that both models can explain the experimentally observed resonant nature of the Raman response. However, we found that the extended Hubbard-Holstein model, including electron-phonon coupling, gives a better description of experimental data. First, the Hubbard-Holstein model, in contrast with the pure Hubbard model, reproduces experimentally observed asymmetry of the Raman spectrum. Second, the presence of the electron-phonon coupling is manifested in experimental visibility of the two-magnon peak in optical conductivity. Finally, the Hubbard-Holstein model predicts correct positions of peaks both in the Raman response and optical conductivity with the same parameters, i.e. it provides a unified description of two spectral properties in a situation where pure Hubbard model fails.

This work was funded by ImPACT Program of Council for Science, Technology and Innovation (Cabinet Office, Government of Japan). Work at the University of Colorado was supported by the NSF under Grant No. DMR-1709946.

[1] P.A. Lee, N. Nagaosa, X.G. Wen, Reviews of Modern Physics **78**(1), 17 (2006)

[2] T.P. Devereaux, A. Virosztek, A. Zawadowski, Phys. Rev. B **51**, 505 (1995)

[3] G. Khaliullin, P. Horsch, Physica C: Superconductivity **282**(Part 3), 1751 (1997)

[4] O. Rösch, O. Gunnarsson, Phys. Rev. Lett. **92**, 146403 (2004)

[5] A.S. Mishchenko, N. Nagaosa, Physical Review Letters **93**(3) (2004)

[6] O. Rösch, O. Gunnarsson, Phys. Rev. Lett. **93**, 237001 (2004)

[7] O. Rösch, O. Gunnarsson, X.J. Zhou, T. Yoshida, T. Sasagawa, A. Fujimori, Z. Hussain, Z.X. Shen, S. Uchida, Phys. Rev. Lett. **95**, 227002 (2005)

[8] G. Sangiovanni, O. Gunnarsson, E. Koch, C. Castellani, M. Capone, Phys. Rev. Lett. **97**, 046404 (2006)

[9] V. Cataudella, G. De Filippis, A.S. Mishchenko, N. Nagaosa, Physical Review Letters **99**(22), 226402 (2007)

[10] A.S. Mishchenko, N. Nagaosa, Z.X. Shen, G. De Filippis, V. Cataudella, T.P. Devereaux, C. Bernhard, K.W. Kim, J. Zaanen, Physical Review Letters **100**(16), 166401 (2008)

[11] F. Novelli, G. De Filippis, V. Cataudella, M. Esposito, I.V. Kausel, F. Cilento, E. Sindici, A. Amaricci, C. Giannetti, D. Prabhakaran, S. Wall, A. Perucchi, S. Dal Conte, G. Cerullo, M. Capone, A. Mishchenko, M. Grninger, N. Nagaosa, F. Parmigiani, D. Fausti, Nature Communications **5**(1), 5112 (2014)

[12] O. Gunnarsson, O. Rsch, Journal of Physics: Condensed Matter **20**(4), 043201 (2008)

[13] A.S. Mishchenko, Phys. Usp. **52**(12), 1193 (2009)

[14] A.S. Mishchenko, N. Nagaosa, K.M. Shen, Z.X. Shen, X.J. Zhou, T.P. Devereaux, EPL **95**(5) (2011)

[15] L. Feiner, J. Jefferson, R. Raimondi, Physical Review B **53**(13), 8751 (1996)

[16] M. Simon, A. Aligia, E. Gagliano, Physical Review B **56**(9), 5637 (1997)

[17] T. Tohyama, H. Onodera, K. Tsutsui, S. Maekawa, Physical Review Letters **89**(25), 257405 (2002)

[18] G. Seibold, C. Castellani, C. Di Castro, M. Grilli, Physical Review B **58**(20), 13506 (1998)

[19] S. Raghu, E. Berg, A. Chubukov, S. Kivelson, Physical Review B **85**(2), 024516 (2012)

[20] Supplemental Material describes methods used in calculations, justifies parameters of the model, and contains references[41–46].

[21] D. Reznik, M.V. Klein, W. Lee, D.M. Ginsberg, S.W. Cheong, Physical Review B **46**(18), 11725 (1992)

[22] M. Yoshida, S. Tajima, N. Koshizuka, S. Tanaka, S. Uchida, T. Itoh, Physical Review B **46**(10), 6505 (1992)

[23] G. Blumberg, P. Abbamonte, M.V. Klein, W.C. Lee, D.M. Ginsberg, L.L. Miller, A. Zibold, Physical Review B **53**(18), R11930 (1996)

[24] A.V. Chubukov, D.M. Frenkel, Physical Review Letters **74**(15), 3057 (1995)

[25] Morr, Dirk K. and Chubukov, Andrey V., Physical Review B **56**(14), 9134 (1997)

[26] Hanamura, Eiichi and Dan, Nguyen Trung and Tanabe, Yukito, Physical Review B **62**(11), 7033 (2000)

[27] The polarization-resolved electronic Raman spectrum intensity at zero temperature as a function of the Raman shift is given in Eqs.(5-6) up to a factor. In order to fit experimental observations in Fig. 1, we have chosen two different factors for $\lambda = 0$ and $\lambda = 0.6$. The two factors differ by 1.9. By varying the incoming frequency (in order to obtain the resonant behavior of Raman response in the $B_{1g} + A_{2g}$ symmetry shown in Fig. 4), this multiplicative contribution has not been changed. The same factors have been used also into the Supplemental Material

[28] N. Chelwani, A. Baum, T. Bohm, M. Opel, F. Venturini, L. Tassini, A. Erb, H. Berger, L. Forr, R. Hackl, arXiv:1705.01496

[29] J. Lorenzana, G.A. Sawatzky, Physical Review B **52**(13), 9576 (1995)

[30] G. De Filippis, V. Cataudella, E.A. Nowadnick, T.P. Devereaux, A.S. Mishchenko, N. Nagaosa, Physical Review Letters **109**(17), 176402 (2012)

[31] J.D. Perkins, J. Graybeal, M. Kastner, R. Birgeneau, J. Falck, M. Greven, Physical Review Letters **71**(10), 1621 (1993)

[32] J. Orenstein, G.A. Thomas, A.J. Millis, S.L. Cooper, D.H. Rapkine, T. Timusk, L.F. Schneemeyer, J.V. Waszczak, Phys. Rev. B **42**, 6342 (1990)

[33] G. Yu, C.H. Lee, D. Mihailovic, A.J. Heeger, C. Fincher, N. Herron, E.M. McCarron, Phys. Rev. B **48**, 7545 (1993)

[34] Cooper, S. L., Kotz, A. L., Karlow, M. A., Klein, M. V., Lee, W. C., Giapintzakis, J. and Ginsberg, D. M., Phys. Rev. B **45**(5), 2549 (1992)

[35] B.S. Shastry, B.I. Shraiman, Physical Review Letters **65**(8), 1068 (1990)

[36] T.P. Devereaux, R. Hackl, Reviews of Modern Physics **79**(1), 175 (2007)

[37] Y. Gallais, I. Paul, Comptes Rendus Physique **17**(1), 113 (2016)

[38] P. Massat, D. Farina, I. Paul, S. Karlsson, P. Strobel, P. Toulemonde, M.A. Méasson, M. Cazayous, A. Sacuto, S. Kasahara, et al., Proceedings of the National Academy of Sciences p. 201606562 (2016)

[39] G. Blumberg, R. Liu, M.V. Klein, W.C. Lee, D.M. Ginsberg, C. Gu, B.W. Veal, B. Dabrowski, Phys. Rev. B **49**, 13295 (1994)

[40] A.W. Sandvik, S. Capponi, D. Poilblanc, E. Dagotto, Physical Review B **57**(14), 8478 (1998). See also references therein.

[41] E. Dagotto, R. Joynt, A. Moreo, S. Bacci, E. Gagliano, Physical Review B **41**(13), 9049 (1990)

[42] G. De Filippis, V. Cataudella, A. Mishchenko, N. Nagaosa, Physical Review Letters **99**(14), 146405 (2007)

[43] K. Shinjo, T. Tohyama, arXiv preprint arXiv:1709.01297 (2017)

[44] D. Marchand, G. De Filippis, V. Cataudella, M. Berciu, N. Nagaosa, N. Prokofev, A. Mishchenko, P. Stamp, Physical Review Letters **105**(26), 266605 (2010)

[45] G. De Filippis, V. Cataudella, A. Mishchenko, N. Nagaosa, Physical Review B **85**(9), 094302 (2012)

[46] B.S. Shastry, B. Sutherland, Physical Review Letters **65**(2), 243 (1990)